# Accessibility of introduced cysteines in chemoreceptor transmembrane helices reveals boundaries interior to bracketing charged residues

THOMAS BOLDOG AND GERALD L. HAZELBAUER

Department of Biochemistry, University of Missouri–Columbia, Columbia, Missouri 65211, USA

(RECEIVED January 28, 2004; FINAL REVISION February 18, 2004; ACCEPTED February 18, 2004)

**Abstract**

Two hydrophobic sequences, 24 and 30 residues long, identify the membrane-spanning segments of chemoreceptor Trg from *Escherichia coli*. As in other related chemoreceptors, these helical sequences are longer than the minimum necessary for an α-helix to span the hydrocarbon region of a biological membrane. Thus, the specific positioning of the segments relative to the hydrophobic part of the membrane cannot be deduced from sequence alone. With the aim of defining the positioning for Trg experimentally, we determined accessibility of a hydrophilic sulfhydryl reagent to cysteines introduced at each position within and immediately outside the two hydrophobic sequences. For both sequences, there was a specific region of uniformly low accessibility, bracketed by regions of substantial accessibility. The two low-accessibility regions were each 19 residues long and were in register in the three-dimensional organization of the transmembrane domain deduced from independent data. None of the four hydrophobic–hydrophilic boundaries for these two membrane-embedded sequences occurred at a charged residue. Instead, they were displaced one to seven residues internal to the charged side chains bracketing the extended hydrophobic sequences. Many hydrophobic sequences, known or predicted to be membrane-spanning, are longer than the minimum necessary helical length, but precise membrane boundaries are known for very few. The cysteine-accessibility approach provides an experimental strategy for determining those boundaries that could be widely applicable.

**Keywords:** bacterial chemoreceptors; transmembrane proteins; cysteine scanning; lipid bilayers; hydrophobic–hydrophilic boundaries

Much is known about the structure and structural changes of the transmembrane chemoreceptors from *Escherichia coli* (Falke and Hazelbauer 2001). However, as is the case for many transmembrane proteins, we do not know the precise boundaries of the protein segments embedded in the hydrophobic environment of the lipid bilayer. Chemoreceptors are transmembrane homodimers that are constructed of extended helical bundles (Fig. 1A). Each monomer in the homodimer has two transmembrane segments, TM1 and TM2, which traverse the cytoplasmic membrane as helices. These two regions contain sequences of exclusively hydrophobic residues longer than the ~20 necessary for a helix to span a biological membrane. For instance, the TM1 and TM2 regions of chemoreceptor Trg are defined by sequences of 30 and 24 hydrophobic residues, respectively.

Transmembrane α-helices are readily predicted in protein sequences by identification of stretches of exclusively or predominantly hydrophobic residues a minimum of ~20 residues in length (Engelman et al. 1986; von Heijne 1992; Jones et al. 1994; Rost et al. 1995). The predictions are based on the 1.5 Å distance between residues in a canonical α-helix and the ~30 Å width of the hydrophobic part of a membrane (Linden et al. 1977; Seelig and Seelig 1980; Wiener and White 1992; White and Wiener 1996). How-

Reprint requests to: Gerald L. Hazelbauer, Department of Biochemistry, University of Missouri–Columbia, 117 Schweitzer Hall, Columbia, MO 65211, USA; e-mail: hazelbauerg@missouri.edu; fax: (573) 882-5635.

Article published online ahead of print. Article and publication date are at http://www.proteinscience.org/cgi/doi/10.1110/ps.04648604.

 

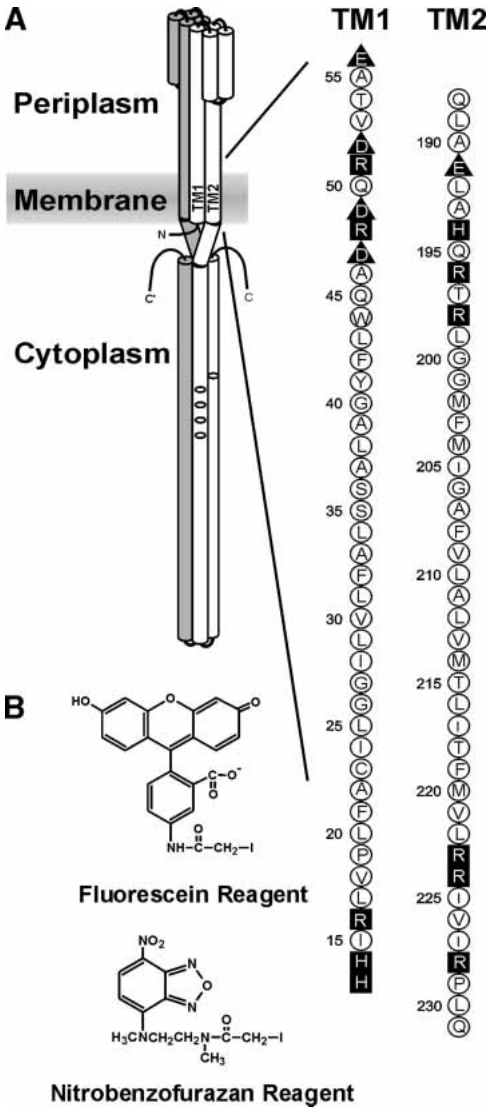


**Figure 1.** Chemoreceptor organization, the transmembrane regions of Trg, and the fluorescent sulfhydryl reagents. (*A*) (*Left*) A cartoon of the organization of a chemoreceptor homodimer. Amino (N) and carboxyl termini (C) are labeled, and one subunit is shaded. On the other subunit, the transmembrane regions TM1 and TM2 are labeled and the positions of methyl-accepting sites shown by ovals. The approximate position of the cytoplasmic membrane is shown as a shaded area. (*Right*) The amino acid sequences (single letter code) of the TM1 and TM2 regions of Trg. Neutral and hydrophobic residues are enclosed in open circles; charged residues, in dark symbols; negative charges, in triangles; and positive charges, in squares. (*B*) Structure of 5-IAF (Fluorescein Reagent) and N, N′-dimethyl-N-(iodoacetyl)-N′-(7-nitrobenz-2-oxa-1, 3-diazol-4-yl)ethylene-diamine (Nitrobenzofurazan Reagent).

ever, many hydrophobic sequences are longer than the minimum. This could reflect a transmembrane helix traversing the membrane at an acute angle and thus having more residues in the hydrophobic environment than a helix normal to the membrane, or some hydrophobic residues might not be embedded in the lipid bilayer. There are a limited number of experimental approaches for determining which specific residues along an extended hydrophobic sequence are actually embedded in the hydrophobic environment of the lipid bilayer. Some require specialized equipment and expertise (Altenbach et al. 1994), and others involve artificial fusion proteins (Monné et al. 1998; Nilsson et al. 1998). In this study we used a convenient and minimally perturbing approach combining cysteine substitutions and determination of accessibility to a hydrophilic sulfhydryl reagent to identify the membrane-embedded segments of chemoreceptor Trg.

## Results

### *Experimental approach*

Our approach is derived from one used by Falke and colleagues to characterize the extra-membrane, cytoplasmic domain of chemoreceptor Tar (Danielson et al. 1997; Bass and Falke 1998; Butler and Falke 1998; Bass et al. 1999; Falke and Kim 2000). They reasoned that substituted cysteines at positions in the native protein at which the side chain was sequestered in the protein interior should be relatively inaccessible to a bulky, water-soluble sulfhydryl reagent such as 5-iodoacetamidofluorescein (5-IAF; Fig. 1B) but cysteines at surface-exposed positions should be relatively accessible. Their experiments revealed periodic variation in relative accessibilities that allowed identification of the helical nature of most of the ~350-residue cytoplasmic domain of the chemoreceptor (Falke and Kim 2000). Could a similar approach distinguish the membrane-embedded from the extra-membrane portions of the helices of Trg? The hydrophobic nature of the lipid bilayer should shield residues from accessibility to a polar sulfhydryl reagent, whether the side chain is packed on other elements of protein structure or exposed on the protein surface. Thus, we determined accessibility to 5-IAF of cysteines introduced at each position within and immediately outside the TM1 and TM2 regions of Trg.

We assembled a set of 88 plasmid-borne *trg* genes coding for Trg containing a single cysteine at positions 13 through 56 and 188 through 231 (Fig. 1A). The first series included and bracketed the exclusively hydrophobic sequence from 17 through 45 that identifies the TM1 region, and the second did the same for the exclusively hydrophobic sequence from 199 through 221 that identifies the TM2 region. Of the 88 altered receptors all but one, with cysteine instead of proline at position 229, were functional as determined in vivo by ability to mediate chemotaxis on a semisolid agar plate. Accessibility experiments were performed by adding a fluorescent sulfhydryl reagent to membrane vesicles containing Trg and allowing the reaction to progress in two conditions, one in which the receptor was left in its native, membrane-embedded state and the other in which the detergent SDS

was added, dissolving the membrane and denaturing the protein, thus providing maximal exposure of the cysteine sulfhydryl to the reagent. After these parallel reactions, samples were submitted to SDS polyacrylamide gel electrophoresis using conditions in which Trg was the only detectable protein at its position in the gel (Fig. 2). Fluorescence intensity of the Trg band was determined by scanning the untreated gel. Then, the relative amount of protein in each Trg band was determined by treating the gel with a fluorescent protein stain and scanning it under conditions in which cysteine-coupled fluorescein did not produce a signal. For each band, intensity of fluorescein fluorescence was normalized to the relative amount of protein. Accessibility was expressed as the ratio of normalized fluorescent labeling for native, membrane-embedded receptor to normalized labeling for SDS-treated material. Values varied from 0 (no accessibility in the native protein) to 1 (identical accessibility in the native, membrane-embedded condition and in the denatured, membrane-dissolved state). Examples of primary data are shown in Figure 2.

### *Accessibility*

We measured accessibility of the negatively charged, fluorescent sulfhydryl reagent 5-IAF to cysteine sulfhydryls at the 88 Trg positions using three independent membrane preparations for each position. In Figure 3, mean values of accessibility with standard deviations are plotted by residue number for the TM1 (Fig. 3A) and TM2 regions (Fig. 3B). For both, there was an extended sequence of very little accessibility (<0.05) to the hydrophilic reagent, flanked by sequences in which many positions exhibited substantially greater accessibility. For the regions of substantial accessibility at the periplasmic ends of both TM1 and TM2, and for much of the cytoplasmic end of TM2, low accessibility alternated with intermediate or high accessibility in a pattern consistent with helical packing. In contrast, at the cytoplasmic end of the TM1 region all positions exhibited accessibilities >0.25, and variation in accessibility did not exhibit periodicity suggestive of a particular secondary structure.

The data identified well-resolved boundaries between hydrophobic and hydrophilic environments. At the cytoplasmic end of the TM1 region, accessibility dropped from >0.25 for positions 13 through 21 to <0.05 for an extended sequence from positions 22 through 40, and increased significantly beginning at position 41 (Fig. 3A). This strongly suggested that the segment of TM1 embedded in the hydrocarbon environment of the membrane was a 19-residue se-

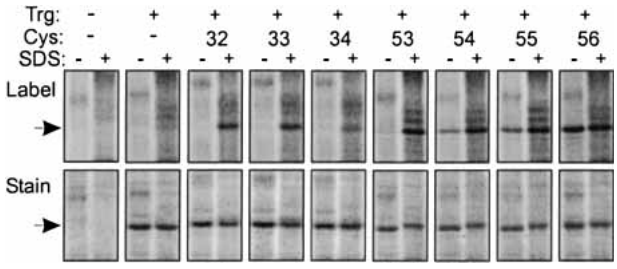


**Figure 2.** Labeling of cysteine-containing forms of Trg by a fluorescent sulfhydryl reagent. Trg lacking cysteine or containing a single cysteine at the indicated positions in the TM1 region was treated with 5-IAF in its native, membrane-embedded state (–) or in the presence of the denaturant and membrane solvent SDS (+), and separated from other proteins in the membrane vesicles by SDS-PAGE. The figure shows two fluorographic images of the same segments of SDS polyacrylamide gels, the *upper* ones generated by fluorescein fluorescence, and the *lower* ones, by the protein stain SYPRO red. The *leftmost* pairs of lanes show patterns for vesicles lacking Trg. The position of Trg, $M_r$ ~60,000, is shown by the arrows.

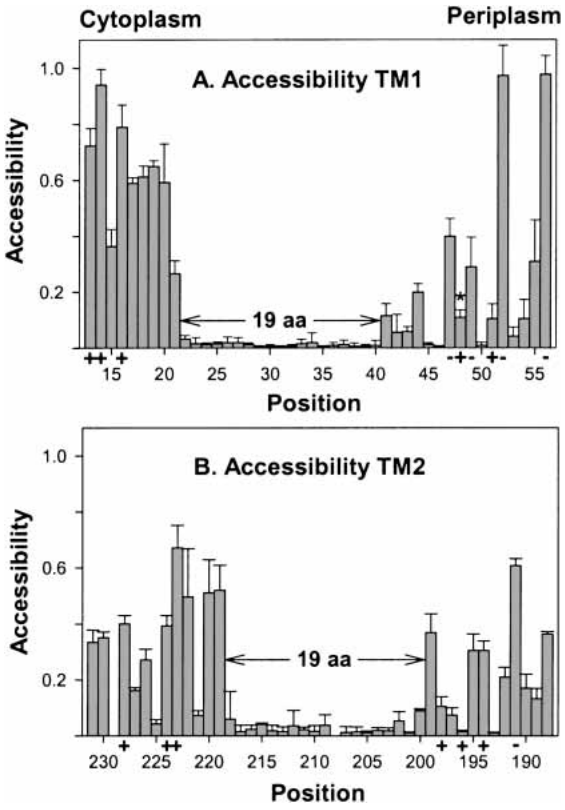


**Figure 3.** Accessibility of introduced cysteines to 5-IAF. Experiments like those in Fig. 2 were performed to determine relative accessibility to 5-IAF of cysteine sulfhydryls at each of the indicated positions in membrane-embedded Trg. Mean values of accessibility (three independent membrane preparations) with standard deviations are plotted by residue number from cytoplasm to periplasm for the TM1 (*A*) and TM2 regions (*B*). Positions of charged residues in the wild-type protein are marked by "+" or "–" along the abscissa, and the sequence of 19 consecutive residues with minimal accessibility is marked by divergent arrows and labeled "19 aa." Position 48 is marked in panel *A* by an asterisk (*) to indicate that the low accessibility is likely the result of bracketing negative charges restricting access by the negatively charged reagent (see text). Because of low receptor content, it was not possible to make reliable measurements for positions 208 and 229.

quence from positions 22 through 40. For the TM2 region, a continuous sequence of very low accessibilities ≤0.05 (positions 201–217) was bracketed at each end by positions with detectably increased but still very modest accessibility on the order of 0.1 (positions 200 and 218, respectively) and by adjacent positions with substantial accessibility, >0.3 (positions 199 and 219, respectively). Accessibility could not be determined for positions 208 and 229 because Trg with a cysteine at either position was present in vesicle preparations at a level too low for reliable measurements. Low content for Trg with cysteine at position 208 had been noted previously (Lee et al. 1995). The low content for position 229 is consistent with the inability of that protein to mediate chemotaxis (see above) and the low content of the analogous cysteine-substituted form of chemoreceptor Tar (Butler and Falke 1998). Receptors with cysteine at positions 200 or 218 were present in vesicles at relatively low levels, and thus quantification required careful definition of the extent of fluorescence above background, but it was clear that there was little accessibility at either position. Even with these limitations, the pattern of accessibilities for the TM2 region provided a straightforward conclusion: The 19-residue sequence from 200 through 218 was the segment of TM2 embedded in the hydrocarbon membrane environment. The slightly increased accessibilities at the two ends of the sequence implied that these residues were modestly accessible to the charged reagent, perhaps as the result of subtle movements of the transmembrane helix in and out of the membrane (see Discussion).

Of the four hydrophobic–hydrophilic interfaces, the periplasmic end of TM1 exhibited the least increase in accessibility on the hydrophilic side of the boundary. Studies of oxidative cross-linking between introduced cysteines (Lee et al. 1994; Hughson et al. 1997; Peach et al. 2002; also see below) indicate that the periplasmic end of TM1 is the helical segment in the transmembrane region exhibiting closest proximity to and greatest number of interactions with neighboring helices. With close helical proximity, access of the bulky, charged 5-IAF could well be limited. We took two approaches to test this idea. In the first approach, we increased concentration and the time of exposure to 5-IAF. For the three positions on the hydrophilic side of the apparent boundary (positions 41–43) the extent of reaction increased; for three on the hydrophobic side (38–40), reaction remained unchanged and essentially undetectable (data not shown). In the second approach, we used a hydrophilic reagent that was smaller than 5-IAF and uncharged. We found that the nitrobenzofurazan sulfhydryl reagent N, N′-dimethyl-N-(iodoacetyl)-N′-(7-nitrobenz-2-oxa-1,3-diazol-4-yl)ethylene-diamine (Fig. 1B) reacted much more extensively in our standard conditions with cysteines at positions 41 and 43 (accessibility >0.5) than did the larger, charged reagent, but still exhibited essentially no reaction for positions 38–40 (data not shown). Thus both approaches supported the location of the hydrophobic–hydrophilic boundary that had been identified by accessibility to 5-IAF in our standard conditions.

We tested accessibility of other positions on the hydrophilic side of the TM1 periplasmic boundary to the nitrobenzofurazan reagent and found a pattern of relative reactivity similar to that for 5-IAF. A striking exception was position 48, for which reactivity with the bulky, negatively charged reagent was low (Fig. 3A), but accessibility by the smaller, neutral reagent was >0.4. This difference implied that the two negatively charged residues that bracket position 48 reduced accessibility to a cysteine that is otherwise solvent-exposed.

### *Patterns of oxidative cross-linking*

Previous studies of the hydrophobic sequences 17–46 and 199–221 had determined relative propensities for oxidative cross-linking between cysteines at homologous positions in the subunits of the Trg homodimer and thus defined helical faces of closest apposition in the transmembrane four-helix bundle (Lee et al. 1994; Hughson et al. 1997). We determined cross-linking propensities for the 88 cysteine-substituted forms of Trg contained in the three membrane preparations used for our accessibility studies (Fig. 4). Several cysteines exhibiting essentially no reactivity with 5-IAF participated in oxidative cross-linking. Thus those cysteines were available for sulfhydryl chemistry, supporting the notion that the lack of reactivity with the charged reagent reflected a membrane-embedded location. Cross-linking results were consistent with previous studies (Lee et al. 1994; Hughson et al. 1997), and extended characterization to bordering hydrophilic regions. Extents of cross-linking across the TM1-TM1′ interface exhibited a distinct helical periodicity from positions 19 through 56, with local maxima defining a helical face of closest apposition between homologous helices (Fig. 5). For the portion not embedded in the membrane (41–56), for which variation in accessibility would be expected to reflect solvent exposure, the face of closest apposition identified by cross-linking maxima was opposite the face defined by maxima in accessibility (Fig. 5), consistent with helical packing of the periplasmic extensions of TM1 and TM1′ (Peach et al. 2002). An exception was position 56, with extensive accessibility and extensive cross-linking. However, this could be understood as the consequence of the separation of subunits in this region (Milburn et al. 1991), allowing accessibility. Cross-linking propensities for positions 13 to 18 at the cytoplasmic end of the TM1 region did not exhibit periodicity, and there was no correlation between accessibility and cross-linking, consistent with the model in which TM1 and TM1′ splay apart toward the cytoplasm (Peach et al. 2002).

For TM2-TM2′, positions of local maxima in cross-linking defined a helical face of closest apposition for positions

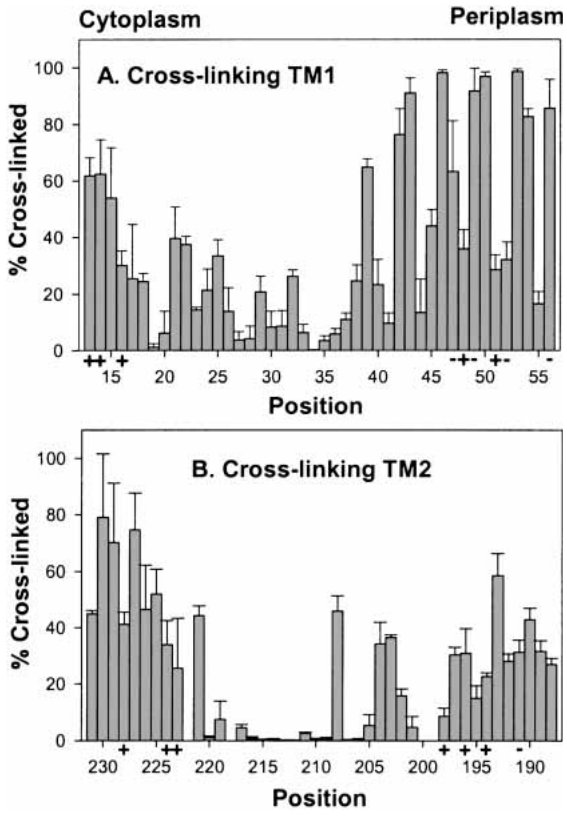


**Figure 4.** Oxidative cross-linking between introduced cysteines. Extent of oxidative cross-linking catalyzed by Cu(phenanthroline)$_3$ was determined for cysteine pairs in homologous positions in the two subunits of the Trg homodimer using the same three membrane preparations used for experiments in Fig. 3. Mean values of percent cross-linking with std. dev. are plotted by residue number displayed from cytoplasm to periplasm for the TM1 (*A*) and TM2 regions (*B*). No data are shown for positions 199, 200, and 222 because of ambiguity in the results.

188 through 208. From 209 to 220, extents of cross-linking were very low, and from 221 through 231 the pattern was not suggestive of a specific secondary structure. The only differences between the current data and the previous study (Lee et al. 1994) occurred in TM2: Cross-linking was higher than observed previously at position 208 and lower at position 211. However, both sets of data identified the same helical face. For the TM2 periplasmic segment with positions accessible to the hydrophilic reagents, variation in homologous cross-linking corresponded with an opposite and complementary variation in accessibility (Fig. 5). However, in the model of the Trg transmembrane domain (Fig. 5), based on extensive cross-linking studies that included analysis of the TM1-TM2 interface (Lee and Hazelbauer 1995), the TM2 face defined by cross-linking maxima is not directly opposite the corresponding face of TM2′ in the receptor dimer. This might reflect inaccuracies in the deduction of structural orientation from patterns of cross-linking. Alternatively, in an array of trimers of receptor dimers, TM2-TM2′ cross-linking might occur between helices from neighboring dimers (Kim et al. 2002; Studdert and Parkinson 2004).

## Discussion

### *Boundaries of TM1 and TM2*

Determination of accessibility of introduced cysteines to a hydrophilic sulfhydryl reagent provided clear identification of the segments of Trg embedded in the hydrophobic environment of the lipid bilayer. For both the TM1 and TM2 regions, there was a continuous stretch of low accessibility 19 residues long, sufficient to span the hydrocarbon environment of the cytoplasmic membrane, a distance measured some years ago as ~30 Å (Linden et al. 1977) and recently estimated to be ~27 Å (Abramson et al. 2003). At all four

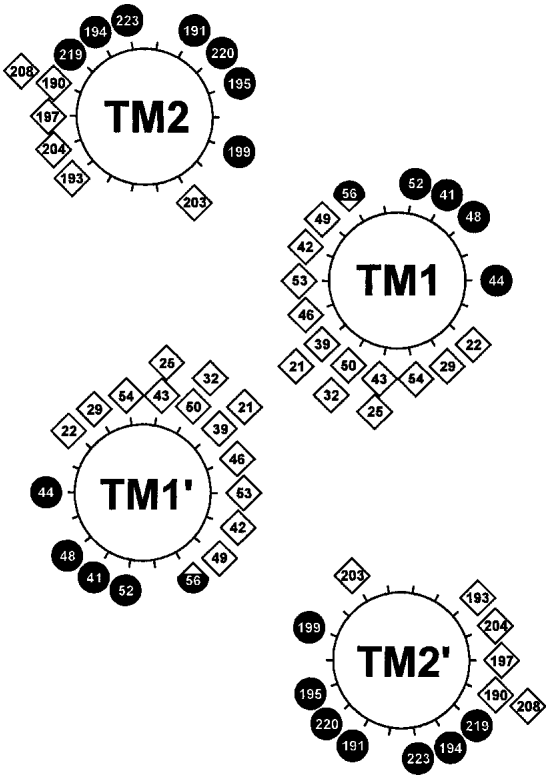


**Figure 5.** Distribution of maxima for accessibility and cross-linking. Local maxima for accessibility from Fig. 3 and for cross-linking from Fig. 4 are displayed as filled circles and open diamonds, respectively, on the helical wheel diagram in the model of the Trg transmembrane domain derived from comprehensive analysis of previous cross-linking data (Lee and Hazelbauer 1995). The local maximum for position 48, which is bracketed by two negatively charged residues, represents high accessibility to an uncharged sulfhydryl reagent, not the lower accessibility for a bulky, charged reagent plotted in Fig. 3A (see text). The hybrid symbol for position 56 reflects local maxima for both cross-linking and accessibility, created by a bulge in helical packing (see text).

hydrophobic–hydrophilic boundaries, there was a distinct transition from very low accessibility to substantially higher accessibility. For TM2, the positions on the hydrophobic side of its two boundaries exhibited modestly increased accessibility, consistent with piston movements of the transmembrane helix in and out of the membrane (Falke and Hazelbauer 2001).

### *Relating the boundaries of two different transmembrane segments*

TM1 and TM2 are parts of the same four-helix transmembrane domain, but our identification of their membrane-embedded segments did not depend on this relationship. Thus an important test was the degree to which those two segments were in register in the complete transmembrane domain. There are no high-resolution structures of the transmembrane domain of Trg, or of any other chemoreceptor. However, we have two sources of information about the relative positions of TM1 and TM2, patterns of oxidative cross-linking between introduced cysteines (Lee et al. 1994; Hughson et al. 1997), and extrapolation from a model of the Trg periplasmic domain (Peach et al. 2002) created from the X-ray structure of the periplasmic domain of the related chemoreceptor Tar (Milburn et al. 1991). Utilizing these two independent sources of information provides somewhat different long-axis positioning of TM1 relative to TM2 (Peach et al. 2002). Because much evidence indicates that there is a piston motion of TM2 along this axis (Falke and Hazelbauer 2001), it seems likely that this difference reflects the natural conformational flexibility of the receptor. Precise alignment of the two 19-residue sequences of low accessibility for TM1 and TM2 of Trg places the two transmembrane helices in a register that is between the two other alignments and closer to the one defined by extrapolation from the X-ray structure (Fig. 6). This correspondence provides confidence in the validity of our analysis and makes it unlikely that a specific cysteine substitution has altered the

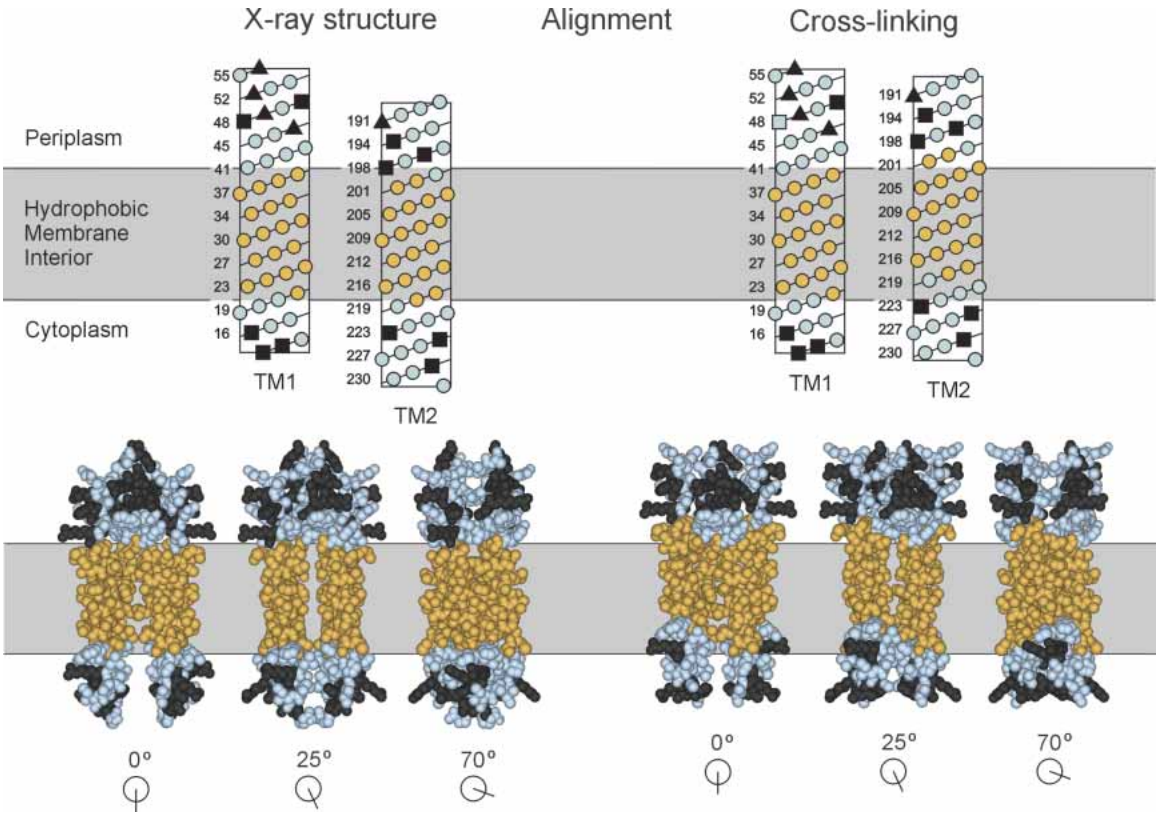


**Figure 6.** Alignment of TM1 and TM2. Positions in TM1 and TM2 exhibiting minimal accessibility to 5-IAF (Fig. 3) are shown in gold, and positions outside this region are in blue. Charged residues, all of which are outside the region of minimal accessibility, are in dark gray. In the *upper* panel, sequences of the TM1 and TM2 regions are displayed in helical net diagrams and aligned along their long axes by two independent criteria. (*Left*) Extension of the homology model based on the X-ray structure of the periplasmic domain of chemoreceptor Tar (Milburn et al. 1991; Peach et al. 2002). (*Right*) Alignment by patterns of oxidative cross-linking between introduced cysteines (Lee et al. 1994; Hughson et al. 1997; Peach et al. 2002). The two alignments are placed relative to the membrane so that in each the minimally accessible positions in TM1 are all in the hydrophobic interior. The *lower* panel presents three space-filling views of the two alignments based on models of the entire transmembrane domain of Trg (Milburn et al. 1991; Peach et al. 2002). The models include TM1/TM1′ residues 13–56 and TM2/TM2′ residues 188–229.

position of that residue relative to the membrane boundary. The combination of cysteine scanning and reagent accessibility could easily be applied to identification of membrane-embedded sequences and specific boundaries of transmembrane domains in other transmembrane proteins. Although not focusing on determination of precise membrane boundaries, the topology study of Stewart and Hermodson (2003) provides an independent example of the ability of this approach to distinguish membrane-embedded from extra-membrane positions.

### *Chemoreceptor organization*

Nineteen-residue sequences organized as canonical α-helices should be 28.5 Å long. Thus the membrane-embedded segments of TM1 and TM2 would need to be oriented normal to the plane of the cytoplasmic membrane to span the ~27–30 Å width of its hydrophobic portion (Linden et al. 1977; Abramson et al. 2003). This implies that Trg, and presumably related chemoreceptors, are oriented normal to the membrane as they span it. This is the orientation shown in most diagrams and cartoons of chemoreceptors (e.g., Fig. 1). Our data provide evidence that this is the case for receptors embedded in their natural membrane environment. High-resolution electron micrographs show the same orientation for chemoreceptor Tsr in membrane fragments treated with low amounts of a nondenaturing detergent (Weis et al. 2003).

To what extent can boundaries for the Trg transmembrane domain be extrapolated to other chemoreceptors? Trg is closely related by sequence to other methyl-accepting chemoreceptors in *E. coli* and *Salmonella* (Bollinger et al. 1984), and these proteins are the most extensively characterized members of a large family of sequence-related, membrane-spanning sensory receptors found across the taxonomic diversity of bacteria and archaea (Zhulin 2001). Figure 7 shows an alignment of the transmembrane regions of chemoreceptors from *E. coli*, *Salmonella*, and the related enteric species *Enterobacter aerogenes*. In all these sequences, residues aligned with the membrane-embedded positions of Trg are exclusively hydrophobic. Thus each of these sequences could be embedded in the hydrocarbon environment of the lipid bilayer. Chemoreceptors, particularly ones as closely related as this set, are likely to have most structural features in common. Thus Figure 7 provides a useful preliminary definition of membrane-embedded segments for other chemoreceptors.

A common feature of transmembrane helices is the presence of aromatic side chains near presumed hydrophobic–hydrophilic boundaries (Ulmschneider and Sansom 2001). Examination of sequences and suggested membrane boundaries in Figure 7 reveals that in the set of these related chemoreceptors an aromatic side chain occurs very frequently near the periplasmic boundary of both transmembrane segments. All but Trg have an aromatic residue at the TM1 membrane-embedded position nearest the periplasm, and the entire set has an aromatic side chain three to five residues from the periplasmic boundary of TM2. In contrast, among the 10 TM1 and 10 TM2 membrane-embedded sequences, only four of 20 have aromatic residues near the cytoplasmic boundary. However, in each receptor sequence an aromatic residue occurs on the extra-membrane side of TM2 cytoplasmic boundary, at the boundary or one residue removed.

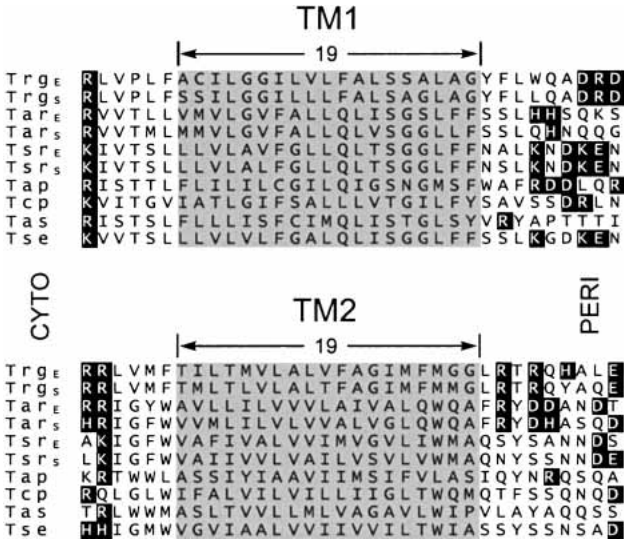


**Figure 7.** Sequence alignments of TM1 and TM2 regions from enteric bacteria. The figure shows the TM1 and TM2 regions of a computer-generated alignment of the complete sequences of chemoreceptors Trg, Tar, and Tsr from *E. coli* and from *Salmonella*, Tap from *E. coli*, Tcp from *Salmonella*, and Tas and Tse from *Enterobacter aerogenes*. There are few residue identities in the regions shown. However, alignment in the TM2 region is the result of extension without gaps from the extensive stretch of residue identity among the sequences over much of the ~350-residue carboxyl terminal domain. Alignment in the TM1 region derives primarily from the correspondence of a cluster of positively charged residues on the amino-terminal side of the extended hydrophobic sequences. Charged residues are in dark boxes, and the segments identified as embedded in the hydrophobic environment for Trg are shaded for all sequences.

### *Extra-membrane segments*

For the short extra-membrane segments analyzed in this study, there were local maxima of accessibility for the TM1 and TM2 periplasmic extensions (Fig. 5). The maxima defined helical faces of high accessibility and thus solvent exposure. Those helical faces were distinct from apposed helical faces defined by maxima for homologous cross-linking between introduced cysteines. Identification of a helical character for the periplasmic extension of TM2 confirmed that the α4 helix of the periplasmic domain (Milburn et al. 1991) is uninterrupted as it becomes TM2 (Pakula and Si-

mon 1992; Lee et al. 1994; Lee and Hazelbauer 1995). The relatively low average values of accessibility for positions 41 through 56 and the distinct helical variation in those values were consistent with the close positioning of TM1 to TM1′ and TM2 deduced from patterns of oxidative cross-linking between introduced cysteines (Lee et al. 1994; Lee and Hazelbauer 1995) and from EPR spectra of spin-labeled cysteines (Barnakov et al. 2002). In the cytoplasmic extension of TM1, positions 13 through 21 exhibited substantial accessibility, and the modest variation in those accessibilities was not suggestive of a specific secondary structure. In addition, extents of cross-linking between homologously placed cysteines in TM1 and TM1′ positions 13 through 20 did not exhibit periodic variation, and there was not a reciprocal relationship between extent of accessibility and extent of cross-linking. These observations are consistent with the high mobility exhibited by EPR spin labels placed at positions 17–20 (Barnakov et al. 2002). Taken together, the data indicate that there is no stable association of the cytoplasmic extension of TM1 with other elements of Trg. The sequence might be helical, but very mobile as the result of a flexible connection with TM1 (residue 19 is a proline), or it might not maintain a fixed structure. This lack of stable association for the cytoplasmic extension of TM1 is consistent with studies of the chemoreceptor Tar (Chen and Koshland Jr. 1995; Chervitz et al. 1995).

### *Membrane boundaries interior to bracketing charges*

None of the four hydrophobic–hydrophilic boundaries we identified for the transmembrane helices of Trg corresponded to the position of a charged residue. Instead, the boundaries were displaced one to seven residues internal to the charged side chain at the ends of the extended hydrophobic sequences (specifically seven and five residues for the periplasmic and cytoplasmic ends of TM1, and one and four residues for the periplasmic and cytoplasmic ends of TM2). The displacement is notable, as charged residues are commonly found at one, and often both, ends of an extended sequence of hydrophobic residues in a putative transmembrane segment, and the frequent presence of a positive charge at the intracellular end of a transmembrane helix has provided a powerful tool for deducing topology of transmembrane helices from sequence (von Heijne 1986). A logical implication of the positive-inside rule is that the positively charged side chain would secure and stabilize the position of the hydrophobic stretch of a transmembrane helix relative to the negatively charged surface of a phospholipid bilayer. Such a role might be thought to require that the hydrocarbon-embedded portion of the transmembrane helix begin immediately adjacent to the charged residue. If this is the case, it does not appear to be crucial for the two Trg helices.

What do these observations mean? Perhaps Trg and presumably other chemoreceptors are atypical, and the displacement of the hydrophobic–hydrophilic boundary from the position of charged residues is not common but instead reflects a specific functional requirement. This could be the case for TM2, because a large body of data identifies the conformational change of transmembrane signaling in chemoreceptors as an axial sliding of that helix (Falke and Hazelbauer 2001). Hydrophobic residues at extra-membrane positions adjacent to the membrane-embedded portion of TM2 would allow axial sliding without imposing the substantial energy barrier that would have to be overcome if the membrane-embedded sequence were tightly bracketed by charged residues. However, TM1 is not thought to slide in the course of transmembrane signaling (Falke and Hazelbauer 2001), and thus the placement of the hydrophobic–hydrophilic boundaries for this transmembrane segment cannot be explained in the context of a functional requirement for axial sliding.

Alternatively, displacement of hydrophobic–hydrophilic boundaries from bracketing charged residues might be relatively common for transmembrane helices, particularly in proteins with extended extra-membrane domains. At present, we do not know whether this is the case, as so few hydrophobic–hydrophilic boundaries have been determined experimentally. This provides a strong motivation for applying our approach to other transmembrane helices.

## Materials and methods

### *Single-cysteine forms of Trg*

We used site-directed mutagenesis (Quick Change, Stratagene) to extend the set of *trg* genes coding for single-cysteine forms of the receptor (Lee et al. 1994) to include the entire sequence from 13 through 56 and 188 through 231. The altered genes were carried in derivatives of pGB1 (Burrows et al. 1989) or pAL1 (Feng et al. 1999) and thus were controlled by a modified *lac* promoter/operator. We introduced each plasmid into a host lacking chromosomal *trg* but otherwise wild type for chemotaxis. Growth without exogenous inducer (pGB1 constructs) or with a low concentration of inducer (pAL1 constructs) results in a cellular content of Trg comparable to that created by a single chromosomal copy of *trg* (Feng et al. 1997). We used these conditions to test the ability of each cysteine-substituted receptor to mediate chemotaxis. Strains were inoculated into a semisolid agar plate containing attractant galactose or ribose, and assessed for the ability to form a chemotactic ring (Lee et al. 1995).

### *Membrane vesicles*

The set of plasmids was introduced into CP553, which lacks chromosomal copies of *tar*, *tsr*, *trg*, *tap*, *cheB*, and *cheR* (Burrows et al. 1989). To prepare membrane vesicles containing each of the single-cysteine forms of Trg, strains harboring the appropriate plasmid were inoculated into 25 mL Luria Broth containing 100 mg/mL ampicillin and incubated at 35°C with agitation. At $OD_{560}$

0.4, isopropyl-thio-β-D-galactoside was added to 1 mM, and incubation continued for 3.5 h. Cells were harvested by centrifugation, suspended in 6 mL 100 mM sodium phosphate (pH 7.0), 10% w/v glycerol, 10 mM N, N′-ethylenediaminetetraacetic acid (EDTA), 50 mM dithiothreitol (DTT), centrifuged again, suspended in 0.9 mL of the same buffer containing freshly added 1 mM phenylmethylsulfonylfluoride (PMSF) and 1,10-phenanthroline, and stored at −20°C. Frozen cell suspensions were thawed on ice, lysed by sonic disruption (six 5-sec bursts with 25-sec pauses) in an ice/salt bath and centrifuged at 16,000*g* in an Eppendorf centrifuge for 10 min at 4°C. Supernatants were centrifuged 10 min, 100,000 rpm, 2°C in a TLA 100.2 rotor; the resulting pellets suspended in 950 μL 20 mM sodium phosphate (pH 7.0), 2 M KCl, 10% w/v glycerol, 10 mM EDTA containing freshly added 1 mM PMSF and 1,10-phenanthroline, and the suspension was centrifuged as previously described. Pelleted membrane was suspended in 60 μL of the previous buffer lacking KCl and containing 1mM EDTA, divided into aliquots, flash-frozen in liquid nitrogen, and stored at −70°C. The concentration of protein in the membrane suspensions was consistently ~20 mg/mL, as determined by the bicinchoninic acid protein assay (Pierce) with bovine serum albumin as the standard. Trg was ~10% of protein in the vesicles.

### *Reaction with hydrophilic sulfhydryl reagents*

Frozen membranes were thawed on ice, diluted with 20 mM sodium phosphate (pH 7.0), 10% w/v glycerol, 1 mM EDTA, 200 mM NaCl to a concentration that would provide ~5 μM Trg in the final reaction mixture, and brought to 25°C. A hydrophilic, cysteine-specific fluorescent reagent was added to the membrane suspension. For all experiments summarized in Figure 3, the reagent was 5-IAF (5-IAF, Molecular Probes) added to a final concentration of 500 μM from a freshly prepared 6.25 mM stock in dimethylformamide. Fluorescein carries a carboxyl group with a $pK_a$ below 5 and a hydroxyl with a $pK_a$ of 6.4. Thus it is negatively charged in our experimental conditions. In a few experiments, the final 5-IAF concentration was 750 μM. For some other experiments, the reagent was N, N′-dimethyl-N-(iodoacetyl)-N′-(7-nitrobenz-2-oxa-1,3-diazol-4-yl)ethylene-diamine (IANBD amide, Molecular Probes), freshly prepared in dimethylformamide. Membrane suspensions to which reagent had been added were divided into two portions, and sodium dodecyl sulfate (SDS) added to one portion to a final concentration of 1%. The SDS-treated portion was incubated 7 min at 95°C, and the other portion 20 min at 25°C. Reactions were stopped by addition of 5 vol of 40 mM tris-hydroxyaminomethane (Tris) (pH 7.8), 16 mM $NaH_2PO_4$, 2% w/v SDS, 10% w/v sucrose, 50 μg/mL bromophenol blue, 120 mM β-mercaptoethanol. Samples were boiled for 5 min and subjected to SDS polyacrylamide gel electrophoresis in conditions that resolved the Trg band from other bands near it, specifically 11% acrylamide, 0.073% bisacrylamide (pH 8.2) (Kehry et al. 1983). Immediately after electrophoresis, wet gels were analyzed for fluorescein fluorescence with a Fujifilm FLA-3000 Imaging System using 473 nm excitation illumination and a <520 nm cut-off filter. After this analysis gels were treated 1 h with the SYPRO red (Molecular Probes) fluorescent protein stain in 10% acetic acid, destained 2 × 10 min in 10% acetic acid and analyzed for SYPRO red fluorescence using 532 nm excitation illumination and a <580 nm cut-off filter. The protein stain could be quantified without interference from fluorescein fluorescence, because in 10% acetic acid, fluorescein is uncharged and does not fluoresce. Intensities of fluorescent bands were quantified using ImageGauge (Fujifilm) software, and values were adjusted for the low level of fluorescence observed for Trg lacking cysteine.

Reactivities for extra-membrane positions on both sides of the membrane (Fig. 3) greater than 0.5, and in some cases close to 1.0, indicated that the hydrophilic sulfhydryl reagent had access to both the inside and the outside of membrane vesicles. It seems likely that this reflects the incompletely sealed nature of the vesicle preparations, as it is well documented that similar preparations exhibit receptor signaling that requires access of a charged ligand to periplasmic domains oriented in the vesicle interior (Danielson et al. 1997; Bass and Falke 1998; Butler and Falke 1998; Bass et al. 1999).

### *Oxidative cross-linking*

Analysis of propensities for oxidative cross-linking catalyzed by $Cu(phenanthroline)_3$ between homologously placed cysteines in the two subunits of the Trg dimer was performed using SDS polyacrylamide gel electrophoresis and immunoblotting as described (Lee et al. 1994). Stained bands were digitized with a Kodak EDAS 290 digital camera system, intensities quantified using TotalLab (Phoretix) software. Percent cross-linking was calculated by dividing the intensity of the cross-linked dimer by the sum of the intensities of monomer and cross-linked dimer.

## Acknowledgments

We thank Angela Lilly for site-specific mutagenesis of *trg*. This work was supported in part by grant GM29963 to G.L.H. from the National Institute of General Medical Sciences.

The publication costs of this article were defrayed in part by payment of page charges. This article must therefore be hereby marked "advertisement" in accordance with 18 USC section 1734 solely to indicate this fact.

## References

Abramson, J., Smirnova, I., Kasho, V., Verner, G., Kaback, H.R., and Iwata, S. 2003. Structure and mechanism of the lactose permease of *Escherichia coli*. *Science* **301:** 610–615.

Altenbach, C., Greenhalgh, D.A., Khorana, H.G., and Hubbell, W.L. 1994. A collision gradient method to determine the immersion depth of nitroxides in lipid bilayers: Application to spin-labeled mutants of bacteriorhodopsin. *Proc. Natl. Acad. Sci.* **91:** 1667–1671.

Barnakov, A., Altenbach, C., Barnakova, L., Hubbell, W.L., and Hazelbauer, G.L. 2002. Site-directed spin labeling of a bacterial chemoreceptor reveals a dynamic, loosely packed transmembrane domain. *Protein Sci.* **11:** 1472–1481.

Bass, R.B. and Falke, J.J. 1998. Detection of a conserved α-helix in the kinase-docking region of the aspartate receptor by cysteine and disulfide scanning. *J. Biol. Chem.* **273:** 25006–25014.

Bass, R.B., Coleman, M.D., and Falke, J.J. 1999. Signaling domain of the aspartate receptor is a helical hairpin with a localized kinase docking surface: Cysteine and disulfide scanning studies. *Biochemistry* **38:** 9317–9327.

Bollinger, J., Park, C., Harayama, S., and Hazelbauer, G.L. 1984. Structure of the Trg protein: Homologies with and differences from other sensory transducers of *Escherichia coli*. *Proc. Natl. Acad. Sci.* **81:** 3287–3291.

Burrows, G.G., Newcomer, M.E., and Hazelbauer, G.L. 1989. Purification of receptor protein Trg by exploiting a property common to chemotactic transducers of *Escherichia coli*. *J. Biol. Chem.* **264:** 17309–17315.

Butler, S.L. and Falke, J.J. 1998. Cysteine and disulfide scanning reveals two amphiphilic helices in the linker region of the aspartate chemoreceptor. *Biochemistry* **37:** 10746–10756.

Chen, X. and Koshland Jr., D.E. 1995. The N-terminal cytoplasmic tail of the aspartate receptor is not essential in signal transduction of bacterial chemotaxis. *J. Biol. Chem.* **270:** 24038–24042.

Chervitz, S.A., Lin, C.M., and Falke, J.J. 1995. Transmembrane signaling by the aspartate receptor: Engineered disulfides reveal static regions of the subunit interface. *Biochemistry* **34:** 9722–9733.

Danielson, M.A., Bass, R.B., and Falke, J.J. 1997. Cysteine and disulfide scanning reveals a regulatory α-helix in the cytoplasmic domain of the aspartate receptor. *J. Biol. Chem.* **272:** 32878–32888.

Engelman, D.M., Steitz, T.A., and Goldman, A. 1986. Identifying nonpolar transbilayer helices in amino acid sequences of membrane proteins. *Annu. Rev. Biophys. Biophys. Chem.* **15:** 321–353.

Falke, J.J. and Hazelbauer, G.L. 2001. Transmembrane signaling in bacterial chemoreceptors. *Trends Biochem. Sci.* **26:** 257–265.

Falke, J.J. and Kim, S.H. 2000. Structure of a conserved receptor domain that regulates kinase activity: The cytoplasmic domain of bacterial taxis receptors. *Curr. Opin. Struct. Biol.* **10:** 462–469.

Feng, X., Baumgartner, J.W., and Hazelbauer, G.L. 1997. High- and low-abundance chemoreceptors in *Escherichia coli*: Differential activities associated with closely related cytoplasmic domains. *J. Bacteriol.* **179:** 6714–6720.

Feng, X., Lilly, A.A., and Hazelbauer, G.L. 1999. Enhanced function conferred on low-abundance chemoreceptor Trg by a methyltransferase-docking site. *J. Bacteriol.* **181:** 3164–3171.

Hughson, A.G., Lee, G.F., and Hazelbauer, G.L. 1997. Analysis of protein structure in intact cells: Crosslinking in vivo between introduced cysteines in the transmembrane domain of a bacterial chemoreceptor. *Protein Sci.* **6:** 315–322.

Jones, D.T., Taylor, W.R., and Thornton, J.M. 1994. A model recognition approach to the prediction of all-helical membrane protein structure and topology. *Biochemistry* **33:** 3038–3049.

Kehry, M.R., Engström, P., Dahlquist, F.W., and Hazelbauer, G.L. 1983. Multiple covalent modifications of Trg, a sensory transducer of *Escherichia coli*. *J. Biol. Chem.* **258:** 5050–5055.

Kim, S.H., Wang, W., and Kim, K.K. 2002. Dynamic and clustering model of bacterial chemotaxis receptors: Structural basis for signaling and high sensitivity. *Proc. Natl. Acad. Sci.* **99:** 11611–11615.

Lee, G.F. and Hazelbauer, G.L. 1995. Quantitative approaches to utilizing mutational analysis and disulfide crosslinking for modeling a transmembrane domain. *Protein Sci.* **4:** 1100–1107.

Lee, G.F., Burrows, G.G., Lebert, M.R., Dutton, D.P., and Hazelbauer, G.L. 1994. Deducing the organization of a transmembrane domain by disulfide cross-linking. The bacterial chemoreceptor Trg. *J. Biol. Chem.* **269:** 29920–29927.

Lee, G.F., Dutton, D.P., and Hazelbauer, G.L. 1995. Identification of functionally important helical faces in transmembrane segments by scanning mutagenesis. *Proc. Natl. Acad. Sci.* **92:** 5416–5420.

Linden, C.D., Blasie, J.K., and Fox, C.F. 1977. A confirmation of the phase behavior of *Escherichia coli* cytoplasmic membrane lipids by X-ray diffraction. *Biochemistry* **16:** 1621–1625.

Milburn, M.V., Prive, G.G., Milligan, D.L., Scott, W.G., Yeh, J., Jancarik, J., Koshland Jr., D.E., and Kim, S.H. 1991. Three-dimensional structures of the ligand-binding domain of the bacterial aspartate receptor with and without a ligand. *Science* **254:** 1342–1347.

Monné, M., Nilsson, I., Johansson, M., Elmhed, N., and von Heijne, G. 1998. Positively and negatively charged residues have different effects on the position in the membrane of a model transmembrane helix. *J. Mol. Biol.* **284:** 1177–1183.

Nilsson, I., Saaf, A., Whitley, P., Gafvelin, G., Waller, C., and von Heijne, G. 1998. Proline-induced disruption of a transmembrane α-helix in its natural environment. *J. Mol. Biol.* **284:** 1165–1175.

Pakula, A.A. and Simon, M.I. 1992. Determination of transmembrane protein structure by disulfide cross-linking: The *Escherichia coli* Tar receptor. *Proc. Natl. Acad. Sci.* **89:** 4144–4148.

Peach, M.L., Hazelbauer, G.L., and Lybrand, T.P. 2002. Modeling the transmembrane domain of bacterial chemoreceptors. *Protein Sci.* **11:** 912–923.

Rost, B., Casadio, R., Fariselli, P., and Sander, C. 1995. Transmembrane helices predicted at 95% accuracy. *Protein Sci.* **4:** 521–533.

Seelig, J. and Seelig, A. 1980. Lipid conformation in model membranes and biological membranes. *Q. Rev. Biophys.* **13:** 19–61.

Stewart, J.B. and Hermodson, M.A. 2003. Topology of RbsC, the membrane component of the *Escherichia coli* ribose transporter. *J. Bacteriol.* **185:** 5234–5239.

Studdert, G.A. and Parkinson, J.S. 2004. Crosslinking snapshots of bacterial chemoreceptor squads. *Proc. Natl. Acad. Sci.* **101:** 2117–2122.

Ulmschneider, M.B. and Sansom, M.S. 2001. Amino acid distributions in integral membrane protein structures. *Biochim. Biophys. Acta* **1512:** 1–14.

von Heijne, G. 1986. The distribution of positively charged residues in bacterial inner membrane proteins correlates with the trans-membrane topology. *EMBO J.* **5:** 3021–3027.

———. 1992. Membrane protein structure prediction. Hydrophobicity analysis and the positive-inside rule. *J. Mol. Biol.* **225:** 487–494.

Weis, R.M., Hirai, T., Chalah, A., Kessel, M., Peters, P.J., and Subramaniam, S. 2003. Electron microscopic analysis of membrane assemblies formed by the bacterial chemotaxis receptor Tsr. *J. Bacteriol.* **185:** 3636–3643.

White, S.H. and Wiener, M.C. 1996. The liquid-crystallographic structure of fluid lipid bilayer membranes. In *Biological membranes: A molecular perspective from computation and experiment* (eds. K.M. Merz Jr. and B. Roux), pp. 127–144. Birkhäuser, Boston.

Wiener, M.C. and White, S.H. 1992. Structure of a fluid dioleoylphosphatidylcholine bilayer determined by joint refinement of X-ray and neutron diffraction data. III. Complete structure. *Biophys. J.* **61:** 437–447.

Zhulin, I.B. 2001. The superfamily of chemotaxis transducers: From physiology to genomics and back. *Adv. Microb. Physiol.* **45:** 157–198.